

Performance analysis of circular polarization X-band microstrip patch antenna combined with conical horn

B. Pratiknyo Adi Mahatmanto¹, Dedi Irawadi¹, Hidayat Gunawan¹, Nugroho Widi Jatmiko¹, Dinari Nikken Sulastrie Sirin¹, Supriyono¹, Suhermanto¹, Bambang Dewandaru², Catur Apriono³

¹Research Center for Satellite Technology, National Research and Innovation Agency (BRIN), Bogor, Indonesia

²Department of Electrical Engineering, Faculty of Engineering, President University, Bekasi, Indonesia

³Department of Electrical Engineering, Faculty of Engineering, Universitas Indonesia, Depok, Indonesia

Article Info

Article history:

Received Oct 2, 2023

Revised Apr 4, 2024

Accepted May 26, 2024

Keywords:

Circular polarization

Conical horn

Microstrip antenna

Parabolic reflector

Satellite

X-band

ABSTRACT

A ground station antenna system features a conical horn attached to a microstrip antenna as an alternate receiving feed antenna. The proposed microstrip antenna has circular polarization and operates in the X-band. The far-field parameters of the antenna are measured after developing and simulating the combination of a conical horn and a microstrip antenna. The modeling results for a microstrip antenna with a conical horn offer a working bandwidth of 930 MHz, spanning frequencies 7.44 GHz to 8.37 GHz. The axial ratio measurements for a microstrip antenna joined with a conical horn produce a working bandwidth of 150 MHz, covering frequencies ranging from 7.72 GHz to 7.87 GHz. The conical horn is attached to a microstrip antenna and has a gain of 15.1 dB. The proposed antenna is designed to meet ground station antenna requirements by pairing it with a parabolic reflector with a diameter of 3.7 meters. The primary focus antenna of the proposed design was chosen. The feed antenna and parabolic reflector should be positioned at a focus point distance of 1110 mm for a total gain of 38.9 dB at 7.8 GHz frequency. The proposed antenna can be applied on X-band remote sensing ground stations as a receiving antenna.

This is an open access article under the [CC BY-SA](#) license.



Corresponding Author:

B. Pratiknyo Adi Mahatmanto

Research Center for Satellite Technology, National Research and Innovation Agency (BRIN)

Bogor, West Java, Indonesia

Email: bpra001@brin.go.id

1. INTRODUCTION

Indonesia, an enormous archipelago, has a remarkably diverse ecology and terrain, along with several geographical challenges, and is vulnerable to natural calamities such as earthquakes, tsunamis, volcanic eruptions, and floods in terms of disaster mitigation [1]. Satellite imaging provides a useful platform for monitoring environmental changes such as deforestation, soil erosion, decreasing water quality, and changes in land cover [2], more prompt and efficient response to serious disasters for damage mapping, initial monitoring, and disaster management. Satellite imageries can help with the planning and monitoring of infrastructure upgrades such as roads, bridges, ports, and airports [3], monitor agriculture, anticipate agricultural production, and identify problems like drought or insect infestations [4], and be used to better understand regional and global climate [5]. Remote sensing satellites have proven to be a very effective and significant tool to collect critical information in a comprehensive, timely, and consistent manner [6].

Satellites in orbit around the earth utilize various sensors to collect remote sensing data, transmitting it to ground stations for reception, analysis, and application across various fields [7]. Understanding the intricate interplay between satellite communication and ground stations is crucial for advancing the development of remote

sensing technologies and applications. This knowledge facilitates the creation of more efficient, reliable, and adaptable ground station systems, essential for tackling increasingly complex challenges [8].

An integral element of satellite communication infrastructure is the ground station's antenna system, responsible for receiving remote sensing data from satellites [9]. This system comprises key components: a parabolic reflector, a metal disc with a reflector shaping the signal's path to the antenna's focal point [10], and the feed antenna, positioned near the focal point to capture and transmit the signal to the receiving system [11]. Typically mounted on a drive system, the antenna can be adjusted in both azimuth and elevation directions for precise satellite tracking. The quality, accuracy, and dependability of these antennas are crucial for obtaining high-quality remote sensing data. This antenna needs to be able to receive signals from a variety of angles and route them precisely to satellites. Using horn antennas, the fundamental limitation is their great physical size. The use of microstrip antennas in ground station systems to replace horn antennas is a significant advancement in satellite communications and remote sensing technologies [12]. Microstrip antennas are smaller, lightweight, and cost-effective than traditional horn antennas; they have become a popular choice in a wide range of applications. A microstrip antenna is a flat antenna composed of a tiny sheet of dielectric placed on a conductive substrate such as copper. This arrangement provides a circuit capable of emitting electromagnetic radiation. This antenna features a flat, compact form, making it easy to place on flat surfaces and a space and design-efficient alternative. Microstrip antennas have the advantage of being significantly more compact than horn antennas, making them more suited for ground stations with limited area. Microstrip antennas are typically less expensive to manufacture and install than horn antennas. Microstrip antennas can be constructed in a range of forms and sizes to meet the needs of certain applications. The use of microstrip antennas in ground stations to replace horn antennas has resulted in substantial advancements in satellite communications and remote sensing technology. This condition enables the use of more efficient antennas in terms of space, cost, and design while still meeting the critical necessity for accurate transmission and reception of satellite signals [13].

Circular polarization finds application in ground station systems operating in X-band frequency channels, and it holds significance in the design of microstrip antenna [14]. One notable benefit is its capacity to mitigate multipath phenomena, commonly observed when signals in the X-band frequency encounter reflections from diverse objects and structures surrounding the ground station. It is also more resistant to reflections, which cause variations in phase and amplitude in the signal, reducing the possibility of interference and distortion in communication.

Microstrip antenna designs employ a variety of techniques, including the employment of truncated, slit, and slot elements in the patch to achieve circular polarization. The radiation element in the truncated approach is in the form of a patch that is cut at the edges, where this cut allows the antenna to produce circular polarization and functions to change the shape of the polarization from linear to circular [15], [16]. Circularly polarized microstrip antennas using a slit approach in which one or more slits in the patch element modify the radiation pattern and polarization from linear to circular [17], [18]. Slit antennas have the advantage of providing flexibility in adjusting orientation and polarization properties. The slot-based microstrip antenna with circular polarization is a patch-shaped radiation element with one or more gaps on its surface that operates as a replacement feed element to produce circular polarization [19], [20].

Proximity coupling and coaxial probe approaches are two methods used in microstrip antenna design to achieve different goals based on the application requirements. The proximity coupling technique is easier than others since it includes inserting passive elements such as patches in the top layer and microstrip lines in the middle layer separated by substrate material. Proximity coupling techniques are employed in a variety of applications, such as circular polarization, bandwidth augmentation, and radiation pattern enhancement [21], [22]. Coaxial probe techniques are more stable in terms of performance than other methods because, once properly installed, the probe tends to maintain the intended performance under a variety of environmental circumstances. Coaxial probe techniques are frequently employed in microstrip antenna feed applications, such as horn feeds, to improve signal entry and exit efficiency [23]–[25].

This research proposed using a conical horn attached to a microstrip antenna as an acquiring feed antenna in a ground station antenna system. The proposed X-band antenna has circular polarization. The technique for producing circular polarization was explained in the previous paragraph. According to simulations, the proposed microstrip antenna design offers a gain of 8.31 dB. The return loss modeling results reveal that the antenna can operate at frequencies ranging from 7.52 GHz to 8.35 GHz, with an axial ratio bandwidth ranging from 7.68 GHz to 7.91 GHz. After designing and simulating the combination of a microstrip antenna along with a conical horn, the far-field parameters of the antenna are measured. The return loss modeling findings for a microstrip antenna featuring a conical horn yield a working bandwidth of 930 MHz, spanning frequencies 7.44 GHz to 8.37 GHz. The axial ratio simulation results for a microstrip antenna along a conical horn yield a working bandwidth of 150 MHz, spanning frequencies of 7.72 GHz to 7.87 GHz. A conical horn attached to a microstrip antenna achieves a gain simulation of 15.1 dB.

The return loss measurements for the conical horn attached to the microstrip antenna yielded an operational bandwidth of 1.07 GHz, which covered the frequency range of 7.6 GHz to 8.67 GHz. The gain measurement findings for the conical horn microstrip antenna are 13.65 dB. To fulfill the ground station receiving antenna requirements, the proposed antenna, the conical horn microstrip, is paired with a 3.7-meter-diameter parabolic reflector. The feeding technique for the parabolic antenna system chosen is the primary focus model. After parameterizing the focus point distance between the parabolic reflector and feed antenna, the optimal distance of 1110 mm was determined, giving a total gain of 38.9 dB at 7.8 GHz. This step demonstrates that the proposed antenna can be utilized as a receiving X-band antenna for joint polar satellite system (JPSS)-1 data reception in the ground stations.

2. METHOD

This section explains how to build the proposed antenna design, which consists of a parabolic reflector, a conical horn antenna, and a microstrip antenna. NPC-H220 is the material used as the microstrip antenna substrate with a thickness of 1.6 mm, copper cladding thickness of 0.035 mm, a loss tangent value of 0.0005, and a relative permittivity value of 2.17. The conical horn antenna is made of aluminum which is approximately 4 mm thick. The parabolic reflector, made of aluminum, is one millimeter deep.

2.1. Microstrip antenna

The microstrip antenna has a square radiation patch. The radiation patch is trimmed in a triangular shape at the two opposite ends, with a slit cut also added. These two techniques, truncated and slit, can be used to create antennas with circular polarization. Truncated shapes can be designed to produce circular polarization by carefully shaping the edges to create a circularly polarized radiation pattern [26], [27]. Circular polarization is achieved when the electric field vector rotates circularly as the wave propagates. Slit shapes can be employed to widen the bandwidth over which the antenna maintains specific polarization characteristics [28], [29]. A slit refers to a narrow opening or cut in the radiating patch, and its specific shape and orientation can have a significant impact on the polarization characteristics of the antenna.

The truncated and slit technique values are calculated using (1) and (2). The power connection to the antenna is made using a coaxial probe technique which is pierced from the back of the antenna, specifically the ground plane side, which penetrates the substrate material until it reaches the square-shaped radiation patch. The (3) is used to calculate the value of the location of the coaxial probe. The ring shape on the edge of the microstrip antenna connects the ground plane to the horn antenna, which are both connected using the vias technique.

$$ls = \frac{wp}{2.72} \quad (1)$$

$$ws = \frac{ls}{10} = \frac{wp}{27.2} \quad (2)$$

$$yo = \frac{wp}{2} \quad (3)$$

$$R = \frac{1.8412 \times c}{2 \times \pi \times f_c} \quad (4)$$

Figure 1(a) presents the front, rear, and side views of a microstrip antenna. The front view shows a radiation patch in the middle and a copper ring at the antenna edge. The rear view shows the ground plane part, which is completely covered in copper, and the side view shows the coaxial probe technique, which serves as a feeder for microstrip antennas. The microstrip antenna has a square patch in a circular substrate with a radius of $r=54$ mm, with the following dimensions: $lc=2.4$ mm, $lt=2.75$ mm, $wp=11.6$ mm, $ws=0.3$ mm, $yo=3$ mm, and $ls=2$ mm, as shown in Figure 1(b). To determine the r value as the inner circle diameter of the conical horn antenna, apply (4) with the center frequency set to 7.8 GHz to obtain the initial r value. However, parameterization is used to alter the microstrip antenna's substrate size, with four times the value of R being the best number.

2.2. Conical horn

A horn antenna produces a focused, directed radiation pattern and is available in various shapes and sizes. A conical horn antenna is a type of antenna with the physical shape of a projecting cone that is commonly employed in communications and radar applications. The conical horn antenna has the shape of a cone that is open at one end and widens at the other. An element used to transmit or receive radio frequency waves is usually present at the open end. These antennas are frequently composed of high-quality metals such as copper

or aluminum to improve conductivity and efficiency. These devices are widely utilized in radar and communications due to their consistent emission pattern.

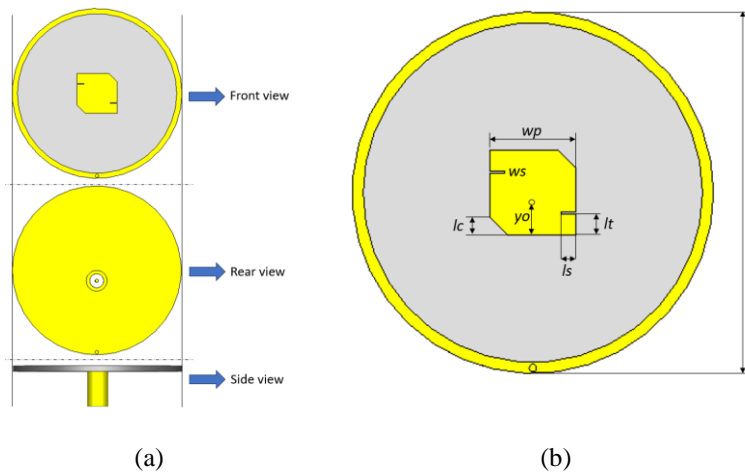


Figure 1. Microstrip antenna from: (a) front view, rear view, and side view and (b) geometry

The (5) is used to calculate the value of the conical horn antenna outer circle (d). In this formula, the frequency 7.8 GHz is used to determine the wavelength value, the value 15 dB is chosen as the expected gain value for the antenna, and L is the loss figure produced by the antenna. After parameterization, the most optimal value for d , 108 mm, is produced. Figure 2(a) is an image of a conical horn from the front with an inner cross-sectional diameter of $d_o=100$ mm and an outer cross-sectional diameter of $d=108$ mm. Figure 2(b) is an image of a conical horn from the back with an inner cross-sectional diameter of $r_o=46$ mm and an outer cross-sectional diameter of $r=54$ mm. Figure 2(c) image of the conical horn from the side with a length of $lh=50$ mm and this value is obtained from (6).

$$d_o = \frac{10^{\left(\frac{G+L}{20}\right)} \lambda}{\pi} \tag{5}$$

$$lh = \frac{d_o^2}{3\lambda} \tag{6}$$

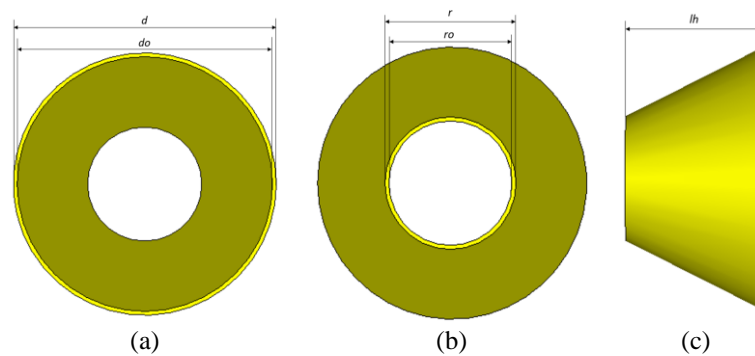


Figure 2. Conical horn from: (a) front view, (b) rear view, and (c) side view

2.3. Parabolic reflector

One type of reflector that concentrates and directs electromagnetic radiation, like radio waves, at a particular spot is a parabolic antenna reflector. The main part of a parabolic antenna is the parabolic reflector, a flat surface that generates the parabola curve. When electromagnetic waves hit the reflector, they are reflected and focused at the parabola's center. The feed antenna is a receiving antenna and an electromagnetic wave

device that is situated close to the center of the parabola. At the focus point, the electromagnetic waves reflected by the parabolic reflector will combine. The antenna feed is placed at the focus point to ensure that the waves are correctly focused. The feed antenna is shown in Figure 3 in paired with a 3.7-meter parabolic reflector. The specifications of the parabolic reflector, as determined from (7), include a diameter of $Di=3700$ mm, a depth of $ho=740$ mm, and a focal point distance of $F=1156.25$ mm.

$$F = \frac{Di^2}{16 ho} \quad (7)$$

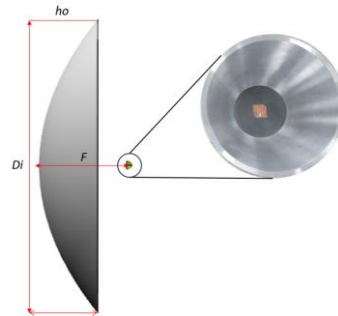


Figure 3. Geometry of 3.7-meter parabolic reflector

3. RESULTS AND DISCUSSION

This section provides an in-depth analysis of the research findings. The collected results include simulation results as well as measurements in the anechoic chamber laboratory. Among the characteristics of the antenna that are mentioned are the return loss, radiation pattern, axial ratio, and gain. The proposed antenna is shown in Figure 4, whose far-field parameters have been measured in the National Research and Innovation Agency (BRIN) anechoic chamber laboratory. Measurement of antenna parameters, including return loss, using the keysight fieldfox microwave analyzer N9917A 18 GHz. Measurements of antenna parameters, including radiation pattern, gain, and polarization, were carried out in an anechoic chamber using a transmit antenna AH systems double ridge guide horn antenna SAS-571 700 MHz-18 GHz and agilent technologies PNA network analyzer N5221A 10 MHz-13.5 GHz device.

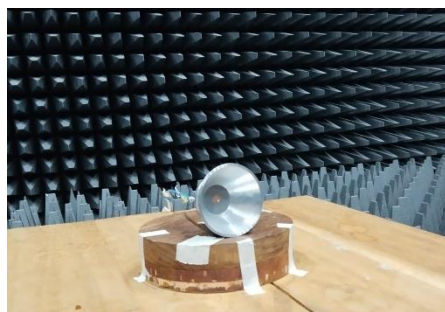


Figure 4. Antenna far-field measurements

3.1. Return loss

Figure 5 presents the comparison results of return loss from three different microstrip antennas: one with a conical horn installed in simulation, and one with a conical horn alongside the antenna in measurement. The microstrip antenna has an 830 MHz bandwidth and operates between 7.52 GHz and 8.35 GHz, with a return loss threshold of -10 dB. In simulation, a microstrip antenna coupled with a conical horn produces a 930 MHz bandwidth with an operating frequency range of 7.44 to 8.37 GHz. In measurement, a microstrip antenna joined with a conical horn produces a 1,070 MHz bandwidth with an operating frequency range of 7.6 to 8.67 GHz. Based on a comparison between the return loss of a single microstrip antenna and a conical horn attached to a microstrip antenna, the microstrip antenna with a conical horn exhibits a larger operating bandwidth than the single microstrip antenna.

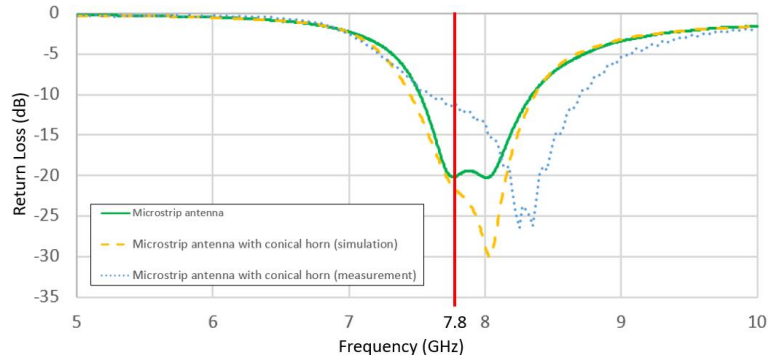


Figure 5. Return loss comparison

Different outcomes are obtained when the return loss of a microstrip antenna coupled with a conical horn is tested and simulated. This result is most likely due to an incorrectly sized patch on the microstrip antenna during antenna manufacturing. As shown in Figure 5, there is erosion in the microstrip patch because the microstrip antenna is designed to operate at the X-band frequency. The size of the antenna is quite small, thus, the little reduced patch size has a significant impact on the form of the ensuing return loss.

3.2. Radiation pattern

Figure 6 shows the E-plane radiation pattern for a microstrip antenna and a conical horn attached to it. A microstrip antenna emits a directional radiation pattern, whereas a conical horn antenna functions as a rectifier, resulting in a more directed radiation pattern. Figure 6 shows back lobes in the 30° and 340° directions, with the microstrip antenna's radiation pattern power ranging from -16 dB to 8 dB. While a conical horn is attached to a microstrip antenna, the radiation pattern becomes more directional, with the primary focus point in a specific direction and a magnitude of approximately 15 dB.

Figure 7 shows the H-plane radiation pattern of a microstrip antenna and a conical horn mounted on it. The microstrip antenna features a directed radiation pattern with a power range of -16 dB to 8 dB. The pattern of radiation of the conical horn antenna is very direct. As a result, when a conical horn is connected to a microstrip antenna, the radiation pattern becomes more directive, with the main concentration of the emission pattern pointing in one direction as in Figure 7. Figures 6 and 7 show noticeable discrepancies between simulation results and measurements of a conical horn attached to a microstrip antenna. This condition occurs because the soldering process on the antenna supply is not neat enough. The second possibility is that the process of manufacturing the conical horn is not smooth enough, resulting in a lot of ripples in the side lobe, resulting in the radiation pattern results during measurement being very different from the radiation pattern results when simulating.

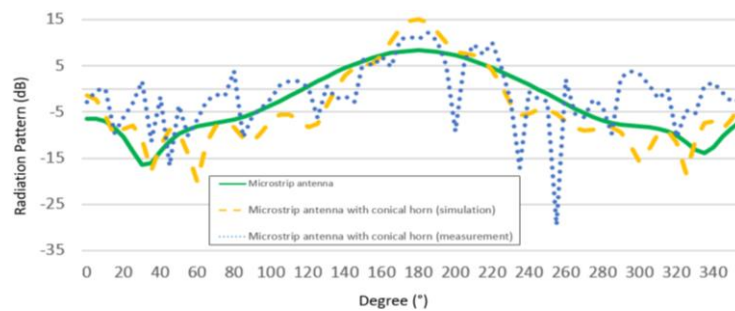


Figure 6. E-plane radiation pattern comparison

3.3. Axial ratio

One of the factors used to assess the level of circularity or ellipticity of polarization on a microstrip antenna designed to produce circular polarization is the axial ratio. This value indicates how close the polarization produced by the antenna is to pure circularity. The electric field vector of the electromagnetic waves generated by the antenna rotates constantly along the circuit in circular polarization.

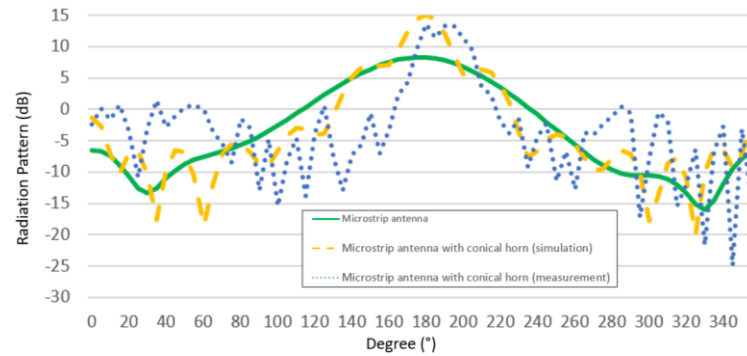


Figure 7. H-plane radiation pattern comparison

As the signal flows forward, the direction of the electric field turns into a circle. Circular polarization has a wide range of uses, particularly in satellite communications and radar. At a given position, the axial ratio is the ratio of the amplitudes of the vertical and horizontal polarization components of the electromagnetic field produced by the antenna. This ratio is used to assess the degree of degeneration from pure circular to elliptical or linear polarization. An axial ratio close to 0 dB suggests near-perfect circular polarization, which is ideal for circular polarization applications.

The axial ratio results for a microstrip antenna with a 3 dB limit range of 7.68 GHz to 7.91 GHz are displayed in Figure 8, yielding a broad axial ratio bandwidth of 230 MHz. In simulation, axial ratio findings for a microstrip antenna coupled with a conical horn using a 3 dB limit range from 7.72 GHz to 7.87 GHz, implying a 150 MHz broad axial ratio bandwidth. In measurement, axial ratio findings for a conical horn attached to a microstrip antenna using a 3 dB limit range from 7.45 GHz to 7.75 GHz, implying a 300 MHz broad axial ratio bandwidth.

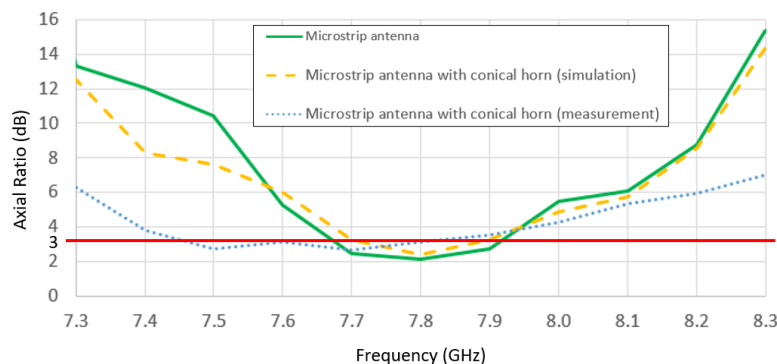


Figure 8. Axial ratio comparison

3.4. Surface current

The surface current simulation on the antenna produces a graphical representation of the surface current flowing across the antenna surface. This simulation is beneficial for understanding and assessing how current flows through the antenna and how the distribution of this current affects the radiation pattern and performance parameters. Surface current simulation visualizes the current distribution across the antenna's surface. It shows where the current is strongest and where it is weak or even zero. This image is often created in the form of a color plot or vector that shows the current direction and amplitude at each location on the antenna.

The current movement in a conical horn attached to a microstrip antenna is depicted in Figures 9(a) to 9(d). The current is moved from the middle of the patch that emerges from the coaxial probe supply to the surface of the radiator, which is a single square patch. These two ways produce a rotating current by using a square patch with cuts at both opposite ends and two slits in the patch facing each other. As illustrated in Figure 9, this antenna creates right hand circular polarization.

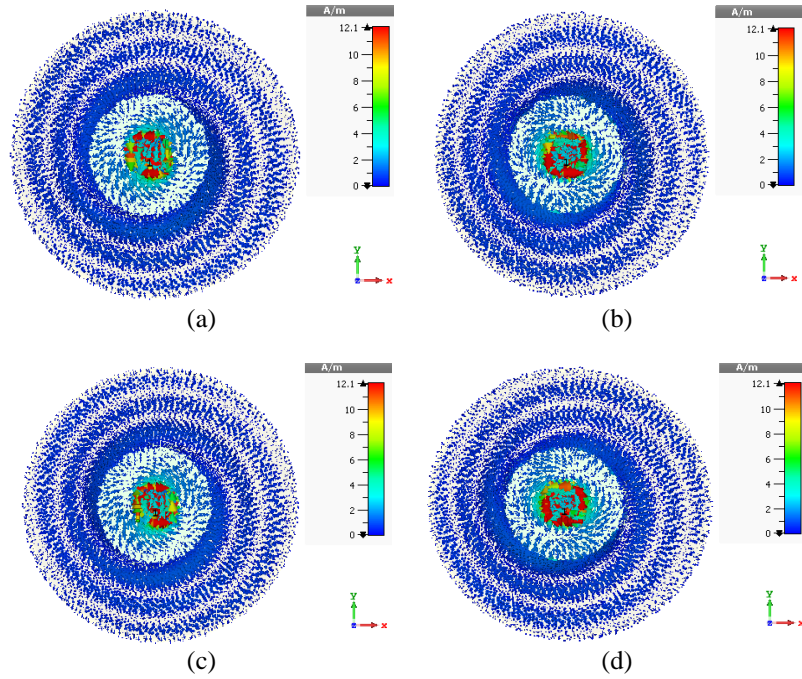


Figure 9. Surface current: (a) 0°, (b) 90°, (c) 180°, and (d) 270°

3.5. Gain antenna

Because satellite reception requires a high antenna gain, a parabolic-shaped reflector could be used to improve the antenna’s gain; however, the point of focus separation between the feeding antenna and the reflector must be taken into consideration. In the prime focus antenna system, the input of the antenna is placed at the parabolic reflector’s middle point of focus. The following phase is to determine the best distance from the source antenna to achieve the best gain value.

Figure 10 presents the parabolic reflector’s focus length parameterization, with an ideal point of focus distance of 1156.25 mm calculated for a 3.7-meter parabolic reflector. At this distance, it generates a gain of 32.1 dB. Due to the required gain being greater than 30 dB, the span between the feeding antenna and the reflector must be specified. Figure 10 shows a characterized image of a parabolic antenna central focus. However, the best results are obtained with a focus length of 1110 mm, resulting in a gain of 38.9 dB.

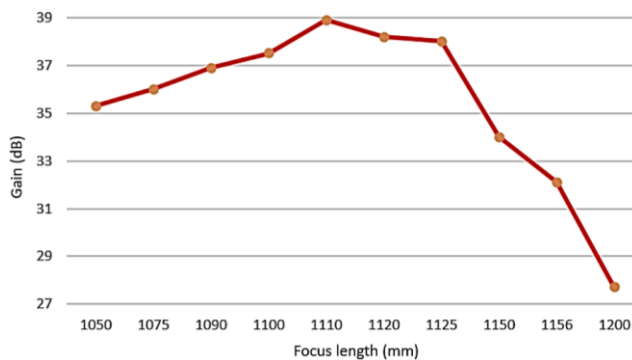


Figure 10. Focus length parameterization at frequency 7.8 GHz

Table 1 compares the gain of the antenna of a microstrip antenna, a conical horn attached to a microstrip antenna, and a feed antenna with a reflector. A microstrip antenna has a gain of 8.31 dB. A conical horn attached to a microstrip antenna achieves a gain of 15.1 dB. Figure 11 depicts a conical horn attached to a microstrip antenna and a 3.7-meter parabolic reflector, with a gain of 38.9 dB. A conical horn attached to a microstrip antenna gives a gain of 15.1 dB. As a result, combining the proposed antenna with a 3.7-meter-

diameter parabolic reflector increases the gain by 23.8 dB. This increase is sufficient to show that the mixed antenna's overall simulation gain encounters the requirements for a satellite gathering antenna at the ground station.

Table 1. Antenna gain comparison

Antenna type	Antenna gain (dB) at 7.8 GHz
Microstrip antenna	8.31
Microstrip antenna with conical horn combined (simulation)	15.10
Microstrip antenna with conical horn combined (measurement)	13.65
Microstrip antenna with conical horn combined 3.7-meter parabolic reflector	38.90

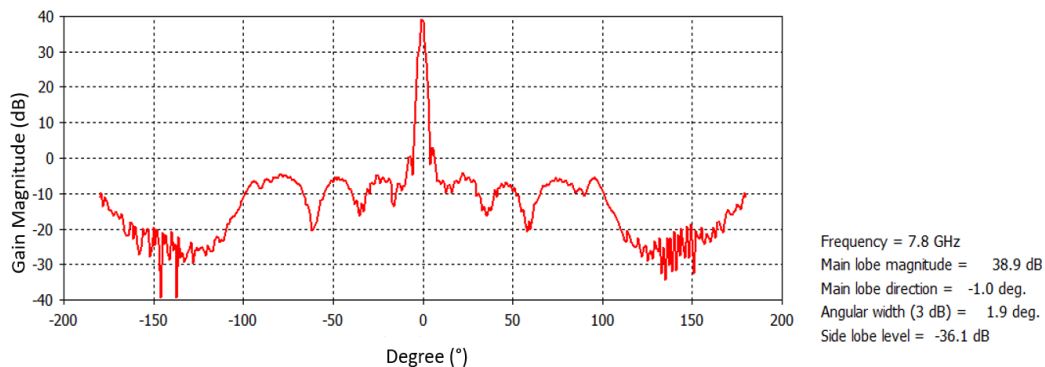


Figure 11. Gain of antenna microstrip with conical horn combined with a 3.7-meter parabolic reflector

Table 2 compares microstrip antennas developed for X-band frequency channels. Kothapudi and Kumar [30], a microstrip antenna with a working frequency of 9.2-9.36 GHz was designed utilizing RT/duroid-5880 material and achieved a gain of 11 dB. The reference paper [31] shows that using RT/Duroid-5880 material to create a microstrip antenna with a working frequency of 9.875-10.125 GHz had a gain of 9.7 dB. In the reference article [32], a gain of 6.08 dB was obtained by employing RO4350B material to create a microstrip antenna with a working frequency of 8.0-8.4 GHz. The proposed antenna, a conical horn attached to a microstrip antenna made of NPC-H220A substrate material, provides a working frequency of 7.44-8.37 GHz and a gain of 15.1 dB.

Table 2. Comparison of microstrip antennas in X-band

Reference	Substrate	Dimension (mm) (lengthxwidthxdepth)	Frequency (GHz)	Gain (dB)
[30]	RT/Duroid-5880	100x100x1.6	9.2-9.36	11
[31]	RT/Duroid-5880	40x40x4.79	9.875-10.125	9.7
[32]	RO4350B	35.6x35.6x3.153	8.0-8.4	6.08
Proposed antenna	NPC-H220A	108x108x52.3	7.44-8.37	15.1

4. CONCLUSION

The proposed microstrip antenna joined with a conical horn has circular polarization and operates in the X-band. The results of the return loss modeling for a microstrip antenna featuring a conical horn produce a working bandwidth of 930 MHz, spanning frequencies 7.44 GHz to 8.37 GHz. The results of an axial ratio simulation for a conical horn attached to a microstrip antenna produce a working bandwidth of 150 MHz, spanning frequencies from 7.72 GHz to 7.87 GHz. The gain simulation result for a conical horn attached to a microstrip antenna is 15.1 dB. The results of return loss parameters, radiation patterns, gain, and axial ratio from simulations and antenna measurements have similar results. The proposed antenna is combined using a 3.7-meter-diameter reflector to fulfill the requirements for receiving antennas at ground stations. The primary focus antenna for the proposed design was chosen. After parameterizing the space between the reflector and the feeding antenna, the optimal distance is 1110 mm, producing a total gain of 38.9 dB at 7.8 GHz frequency. The radiation pattern in the E-plane and H-plane, as well as the antenna return loss and gain, are all considered suitable for use as ground station antennas. Considering the communication system from the JPSS-1 satellite to the ground station requires a bandwidth of 50 MHz, the proposed antenna meets the specifications.

ACKNOWLEDGEMENTS

This research is supported by Faculty of Engineering, Universitas Indonesia through the Professor and Associate Professor of Faculty of Engineering 2023-2024 Seed Funding Grant, under grant number NKB-2566/UN2.F4.D/PPM.00.00/2023 and Research Organization for Aeronautics and Space (ORPA), National Research and Innovation Agency (BRIN) through SK ORPA BRIN No.31/III.1/HK/2023 (PP.5.04).




REFERENCES

- [1] M. Fuady, R. Munadi, and M. A. K. Fuady, "Disaster mitigation in Indonesia: between plans and reality," *IOP Conference Series: Materials Science and Engineering*, vol. 1087, no. 1, p. 012011, Feb. 2021, doi: 10.1088/1757-899x/1087/1/012011.
- [2] J. Li, Y. Pei, S. Zhao, R. Xiao, X. Sang, and C. Zhang, "A review of remote sensing for environmental monitoring in China," *Remote Sensing*, vol. 12, no. 7, p. 1130, Apr. 2020, doi: 10.3390/rs12071130.
- [3] V. Gagliardi *et al.*, "Satellite Remote sensing and non-destructive testing methods for transport infrastructure monitoring: advances, challenges and perspectives," *Remote Sensing*, vol. 15, no. 2, p. 418, Jan. 2023, doi: 10.3390/rs15020418.
- [4] T. Talaviya, D. Shah, N. Patel, H. Yagnik, and M. Shah, "Implementation of artificial intelligence in agriculture for optimisation of irrigation and application of pesticides and herbicides," *Artificial Intelligence in Agriculture*, vol. 4, pp. 58–73, 2020, doi: 10.1016/j.aiaa.2020.04.002.
- [5] H. D. Guo, L. Zhang, and L. W. Zhu, "Earth observation big data for climate change research," *Advances in Climate Change Research*, vol. 6, no. 2, pp. 108–117, Jun. 2015, doi: 10.1016/j.accre.2015.09.007.
- [6] B. Zhang *et al.*, "Progress and challenges in intelligent remote sensing satellite systems," *IEEE Journal of Selected Topics in Applied Earth Observations and Remote Sensing*, vol. 15, pp. 1814–1822, 2022, doi: 10.1109/JSTARS.2022.3148139.
- [7] A. S. Nasution, N. Setyasaputra, W. Sunarmodo, H. Gunawan, and A. Widipaminto, "Integration review of national remote sensing ground station based on virtual ground station by full remote and nearly automation," *IOP Conference Series: Earth and Environmental Science*, vol. 280, no. 1, p. 012029, Aug. 2019, doi: 10.1088/1755-1315/280/1/012029.
- [8] N. S. A. Rahman and N. A. Rahim, "Sustainable framework for a geostationary satellite control earth station system using parallel configuration," *Indonesian Journal of Electrical Engineering and Computer Science*, vol. 30, no. 3, pp. 1498–1508, Jun. 2023, doi: 10.11591/ijeecs.v30.i3.pp1498-1508.
- [9] C. Apriono, B. P. A. Mahatmanto, and F. H. Juwono, "Rectangular microstrip array feed antenna for C-band satellite communications: preliminary results," *Remote Sensing*, vol. 15, no. 4, p. 1126, Feb. 2023, doi: 10.3390/rs15041126.
- [10] B. P. A. Mahatmanto and C. Apriono, "Gain Performance analysis of a parabolic reflector fed with a rectangular microstrip array antenna," in *Proceedings-2020 IEEE International Conference on Industry 4.0, Artificial Intelligence, and Communications Technology*, Jul. 2020, pp. 142–145, doi: 10.1109/IAICT50021.2020.9172035.
- [11] S. S. Roy *et al.*, "Dual band (S-X) ground station antenna for low earth orbit (LEO) satellite tracking application," *IEEE Access*, vol. 10, pp. 80910–80917, 2022, doi: 10.1109/ACCESS.2022.3190417.
- [12] B. P. A. Mahatmanto and C. Apriono, "Rectangular configuration microstrip array antenna for C-band ground station," in *Proceedings of the 2020 27th International Conference on Telecommunications*, Oct. 2020, pp. 1–5, doi: 10.1109/ICT49546.2020.9239576.
- [13] R. J. Kavitha and H. S. Aravinda, "Reviewing the effectiveness of contribution of microstrip antenna in the communication system," *Open Journal of Antennas and Propagation*, vol. 05, no. 02, pp. 47–62, 2017, doi: 10.4236/ojapr.2017.52005.
- [14] U. S. Yudhotomo, S. Salsabilla, Khaerudin, and T. Siahaan, "2.2 GHz S-band helical antenna design for earth surveillance LAPAN-TUBSAT data acquisition in indonesia regional security," *International Journal of Research and Innovation in Applied Science*, vol. 07, no. 11, pp. 43–49, 2022, doi: 10.51584/ijrias.2022.71103.
- [15] X. J. Lin, Z. H. Wu, and Y. Zhang, "A compact triple-band and dual-sense circularly polarized truncated patch antenna," *IEEE Access*, vol. 11, pp. 44287–44293, 2023, doi: 10.1109/ACCESS.2023.3273114.
- [16] Sakshi and M. Bharti, "Corner truncated rectangular MSA with circular polarization," in *IET Conference Proceedings*, 2023, vol. 2023, no. 5, pp. 121–125, doi: 10.1049/icp.2023.1477.
- [17] F. Kurniawan, J. T. S. Sumantyo, A. S. Budianta, D. Hidayat, and Yohandri, "Effect of bended feeding line to the axial ratio on circular patch antenna with triangle truncated," in *IEEE Region 10 Annual International Conference, Proceedings/TENCON*, Oct. 2018, vol. 2018-October, pp. 338–341, doi: 10.1109/TENCON.2018.8650403.
- [18] F. Kurniawan, J. T. S. Sumantyo, P. P. Sitompul, G. S. Prabowo, A. Aribowo, and A. Bintoro, "Comparison design of X-band microstrip antenna for SAR application," in *Progress in Electromagnetics Research Symposium*, Aug. 2018, pp. 854–857, doi: 10.23919/PIERS.2018.8598014.
- [19] M. P. Singh, J. Hirokawa, and S. Ghosh, "A double layer cross-slot aperture-fed millimeter-wave antenna array with wide axial ratio bandwidth," *IEEE Access*, vol. 11, pp. 68550–68559, 2023, doi: 10.1109/ACCESS.2023.3292529.
- [20] J. Lu *et al.*, "A wideband circularly polarized periodic leaky-wave antenna using a novel unit cell with X-shaped slot," *IEEE Transactions on Antennas and Propagation*, vol. 71, no. 8, pp. 6639–6651, Aug. 2023, doi: 10.1109/TAP.2023.3284001.
- [21] C. E. Santosa and J. T. S. Sumantyo, "Design of broadband X-band subarray antenna with hybrid-sequential rotation fed for airborne CP-SAR," in *Proceedings-2021 7th Asia-Pacific Conference on Synthetic Aperture Radar*, Nov. 2021, pp. 1–4, doi: 10.1109/APSAR52370.2021.9688346.
- [22] C. E. Santosa and J. T. S. Sumantyo, "Conformal subarray antenna for circularly polarized synthetic aperture radar onboard UAV," in *2020 International Symposium on Antennas and Propagation*, Jan. 2021, pp. 685–686, doi: 10.23919/ISAP47053.2021.9391362.
- [23] V. Midtboen, K. G. Kjølgaard, and T. S. Lande, "3D printed horn antenna with PCB microstrip feed for UWB radar applications," in *2017 IEEE MTT-S International Microwave Workshop Series on Advanced Materials and Processes for RF and THz Applications*, Sep. 2018, vol. 2018-January, pp. 1–3, doi: 10.1109/IMWS-AMP.2017.8247374.
- [24] B. P. A. Mahatmanto *et al.*, "Design of Circular Polarization Microstrip Patch Antenna Combined with Conical Horn," in *Proceeding-2022 International Conference on Radar, Antenna, Microwave, Electronics, and Telecommunications: Emerging Science and Industrial Innovation in Electronics and Telecommunication*, Dec. 2022, pp. 244–247, doi: 10.1109/ICRAMET56917.2022.9991200.
- [25] A. Mehrdadian and K. Forooghi, "Design and fabrication of a novel ultrawideband combined antenna," *IEEE Antennas and Wireless Propagation Letters*, vol. 13, pp. 95–98, 2014, doi: 10.1109/LAWP.2013.2296559.
- [26] T. Lou, X. X. Yang, Q. D. Cao, and S. Gao, "A low profile circularly polarized beam scanning patch array fed by parallel plate waveguide," *IEEE Transactions on Antennas and Propagation*, vol. 70, no. 9, pp. 7384–7392, Sep. 2022, doi: 10.1109/TAP.2022.3167807.
- [27] F. Kurniawan, J. T. S. Sumantyo, and A. Munir, "Wideband LHCP truncated-circular-shape microstrip antenna for SAR




- application,” in *2017 IEEE Antennas and Propagation Society International Symposium, Proceedings*, Jul. 2017, vol. 2017-January, pp. 2299–2300, doi: 10.1109/APUSNCURSINRSM.2017.8073192.
- [28] M. R. Basar, M. Al-Amin, E. Mirza, P. P. Debnath, and M. R. Awal, “A 2 shape slot microstrip patch antenna for global positioning system satellite communication applications,” *Indonesian Journal of Electrical Engineering and Computer Science*, vol. 31, no. 3, pp. 1392–1399, Sep. 2023, doi: 10.11591/ijeecs.v31.i3.pp1392-1399.
- [29] M. F. Ahmed, A. Z. M. T. Islam, and M. H. Kabir, “Rectangular microstrip antenna design with multi-slotted patch and partial grounding for performance enhancement,” *International Journal of Electrical and Computer Engineering*, vol. 12, no. 4, pp. 3859–3868, Aug. 2022, doi: 10.11591/ijece.v12i4.pp3859-3868.
- [30] V. K. Kothapudi and V. Kumar, “A single layer S/X-band series-fed shared aperture antenna for SAR applications,” *Progress In Electromagnetics Research C*, vol. 76, pp. 207–219, 2017, doi: 10.2528/PIERC17070104.
- [31] M. AlyAboul-Dahab, H. H. M. Ghouz, and A. Z. A. Zaki, “High Gain Compact Microstrip Patch Antenna for X-Band Applications,” *SSRN Electronic Journal*, 2019, doi: 10.2139/ssrn.3441580.
- [32] F. Khairullah and T. Hariyadi, “Design of X-band microstrip antenna for circularly polarized synthetic aperture radar (CP-SAR) system,” in *Proceeding-2020 3rd International Conference on Vocational Education and Electrical Engineering: Strengthening the framework of Society 5.0 through Innovations in Education, Electrical, Engineering and Informatics Engineering*, Oct. 2020, pp. 1–5, doi: 10.1109/ICVEE50212.2020.9243280.

BIOGRAPHIES OF AUTHORS






B. Pratiknyo Adi Mahatmanto    received a B.Eng degree in Electrical Engineering from the Telkom University, Bandung, Indonesia, in 2009 and an M.Eng degree in Electrical Engineering from the Universitas Indonesia, Depok, Indonesia, in 2020. Now, he works as a researcher at the Research Center for Satellite Technology, National Research and Innovation Agency (BRIN). He can be contacted at email: bpra001@brin.go.id.






Dedi Irawadi    received a Bachelor of Science degree in Electrical Engineering from Texas A&M University, College Station, Texas, USA, in 1991. Now, he works as a researcher at the Research Center for Satellite Technology, National Research and Innovation Agency (BRIN). He can be contacted at email: dedi004@brin.go.id.






Hidayat Gunawan    received the B.Eng and M.Eng degrees in Electrical Engineering from Kansai University, Osaka, Japan, in 1992 and 1994, respectively. Now, he works as a researcher of remote sensing ground station technology at the Research Centre of Satellite Technology, Research Organization of Aeronautics and Space (ORPA), Indonesian National Research and Innovation Agency (BRIN). He can be contacted at email: hida003@brin.go.id.



Nugroho Widi Jatmiko    received a Graduate degree in Electrical Engineering from the Universitas Brawijaya, Malang, Indonesia, in 2003 and a Magister degree in Microelectronics and Solid State Electronics from the Beihang University, Beijing, P. R. China, in 2011. Now, he works as a researcher at the Research Center for Satellite Technology, National Research and Innovation Agency (BRIN). He can be contacted at email: nugr003@brin.go.id.






Dinari Nikken Sulastrie Sirin    received a Graduate degree in Electrical Engineering from the Universitas Gadjah Mada, The Special Region of Yogyakarta, Indonesia, in 2004 and the Magister degree in Electrical Engineering from the Universitas Indonesia, Depok, Indonesia, in 2022. Now, she works as a researcher at the Research Center for Satellite Technology, National Research and Innovation Agency (BRIN). She can be contacted at email: dina005@brin.go.id.






Supriyono    received a Graduate degree in Physics Instrumentation from the Universitas Indonesia, Depok, Indonesia, in 1991 and a Magister degree in Electrical and Electronic Engineering from the Universitas Indonesia, Depok, Indonesia, in 1998. Now, he works as a researcher at the Research Center for Satellite Technology, National Research and Innovation Agency (BRIN). He can be contacted at email: supr010@brin.go.id.






Suhermanto    received a Graduate degree in Electrical Engineering from the Universitas Gadjah Mada, The Special Region of Yogyakarta, Indonesia, in 1986 and the Magister degree in Optoelectrotechnics and Laser Applications from the Universitas Indonesia, Depok, Indonesia, in 1998. Now, he works as a researcher at the Research Center for Satellite Technology, National Research and Innovation Agency (BRIN). He can be contacted at email: suhe010@brin.go.id



Bambang Dewandaru    received a B.Eng degree in Telecommunication Engineering from Institut Teknologi Bandung (ITB), Bandung, Indonesia 1981. He received a Master of Science in Electrical Engineering (MSEE) degree from Northeastern University (NU), Boston, Massachusetts, USA in 1993. He received a Doctoral degree in Telecommunication Engineering from the Electrical Engineering Department of Universitas Indonesia (UI), Depok, Indonesia, 2020. He has experience working as General Manager of Marketing and Business Development of TELKOM's Regional Asia Pacific PALAPA satellite communication network. He has experience working as Director for Planning and Construction of the PT Multimedia Nusantara. Now, he works as a Coordinator Lecturer of Electrical Engineering Study program, at President University. He can be contacted at email: bambang.dewandaru@ieee.org.



Catur Apriono    received the B.Eng and M.Eng degrees in Telecommunication Engineering from the Department of Electrical Engineering, Universitas Indonesia, Indonesia, in 2009 and 2011, respectively, and the Ph.D degree in nano vision technology from Shizuoka University, Japan, in 2015. Since 2018, he has been an Associate Professor of Telecommunication Engineering with Universitas Indonesia, where he is currently a researcher and lecturer with the Department of Electrical Engineering, Faculty of Engineering. His current research interests include antenna and microwave engineering, terahertz wave technology, and optical communications. He has been a member of the IEEE Antenna and Propagation Society (AP-S) and the IEEE Microwave Theory and Technique Society (MTT-S). He can be contacted at email: catur@eng.ui.ac.id.